JACC: CARDIOVASCULAR IMAGING
VOL. 9, NO. 7, 2016

ISSN 1936-878X/$36.00
PUBLISHED BY ELSEVIER
http://dx.doi.org/10.1016/j.jcmg.2016.05.003

iREVIEWS

STATE-OF-THE-ART PAPERS

The Remarkable 50 Years of Imaging in HCM and How it Has Changed Diagnosis and Management

From M-Mode Echocardiography to CMR

Barry J. Maron, MD, Martin S. Maron, MD

ABSTRACT

The almost 50-year odyssey of cardiac imaging in hypertrophic cardiomyopathy (HCM), revisited and described here, has been remarkable, particularly when viewed in the timeline of advances that occurred during a single generation of investigators. At each step along the way, from M-mode to 2-dimensional echocardiography to Doppler imaging, and finally over the last 10 years with the emergence of high-resolution tomographic cardiac magnetic resonance (CMR), evolution of the images generated by each new technology constituted a paradigm change over what was previously available. Together, these advances have transformed the noninvasive diagnosis and management of HCM in a number of important clinical respects. These changes include a more complete definition of the phenotype, resulting in more reliable clinical identification of patients and family members, defining mechanisms (and magnitude) of left ventricular outflow obstruction, and novel myocardial tissue characterization (including in vivo detection of fibrosis/scarring); notably, these advances afford more precise recognition of at-risk patients who are potential candidates for life-saving primary prevention defibrillator therapy. This evolution in imaging as applied to HCM has indelibly changed cardiovascular practice for this morphologically and clinically complex genetic disease. (J Am Coll Cardiol Img 2016;9:858–72)

Since the initial description of hypertrophic cardiomyopathy (HCM) >50 years ago, most of our understanding of this complex and heterogeneous genetic heart disease has resulted from insights gained through advances in cardiovascular imaging techniques. Indeed, perhaps no other heart disease has been so uniquely suited to noninvasive imaging as HCM (1-10). In many respects, the development of cardiac imaging from M-mode echocardiography to cardiac magnetic resonance (CMR) transpiring over several decades has paralleled the evolving understanding of this clinically and morphologically diverse disease (**Figures 1 and 2**). Therefore, in this comprehensive historical review, we revisit the development of imaging technology to assess its impact on the diagnosis and management of HCM (10).

THE BEGINNING

In the early 1960s, Dr. Harvey Feigenbaum (Indianapolis, Indiana) was largely responsible for the clinical adaptation of cardiac ultrasound (which he

From the Hypertrophic Cardiomyopathy Institute, Tufts Medical Center, Division of Cardiology, Boston, Massachusetts. Dr. Barry J. Maron was formerly at the Hypertrophic Cardiomyopathy Center, Minneapolis Heart Institute Foundation, Minneapolis, Minnesota. Both authors have reported that they have no relationships relevant to the contents of this paper to disclose.

Manuscript received February 10, 2016; revised manuscript received May 2, 2016, accepted May 12, 2016.

termed "echocardiography") (11–15), due to his vision, energy and focus, and fervent belief in this new technology. Dr. Feigenbaum formulated a worldwide initiative that included publications, workshops, national/international conferences, a comprehensive textbook spanning 45 years, the first commercially available sector scanner, and a cadre of trainees who carried forth a new message to a skeptical establishment.

Early investigations from the Feigenbaum laboratory reported the capability of measuring left ventricular (LV) wall thickness and cavity dimensions, and recognition of the ventricular septum (12,14–16). These observations and those of other investigators (17,18) were instrumental in promoting the imaging revolution for cardiac diseases (prominently including HCM).

EARLY HISTORICAL PERSPECTIVES ON CARDIAC/HCM DIAGNOSES

The initial contemporary morphologic description of HCM was recorded in 1958 by Dr. Donald Teare, the Coroner of London (19). In 8 young patients who had died suddenly, Dr. Teare described the classic gross and histologic features of HCM, including the asymmetric pattern of left ventricular hypertrophy (LVH) that ultimately became a diagnostic marker in the imaging era (20). Although these findings were considered possibly those of a cardiac tumor, his report is remarkable because it described for the first time, in novel anatomic detail, the disease entity that became HCM.

In the decade that followed (1960 to 1970), clinical recognition and investigation of HCM began in earnest, dominated by the Braunwald group at the National Institutes of Health (Bethesda, Maryland) (1). Their findings were largely hemodynamic and angiographic observations (**Central Illustration**) in the cardiac catheterization laboratory but also involved electrocardiograms, history-taking, and precordial auscultation. In 1958, a young man with a subaortic gradient and malignant family history became the first patient clinically diagnosed with HCM (21).

ECHOCARDIOGRAPHY AND M-MODE IMAGING. Introduction of echocardiography to clinical practice in the early 1970s signaled an abrupt transition from invasive cardiac catheterization to the modern imaging era (4,6,9,22,23) (**Central Illustration**). M-mode, a time-motion technique ("M" for motion), provided a single-dimensional ("ice pick") representation of the heart (3,11,12,22,23) directed blindly through narrow rib interspaces, dissecting the center of the LV cavity to avoid obliquity. Consequently, images of the LV wall were confined to a small portion of the basal anterior ventricular septum and posterior (inferior) LV free wall (**Figure 3**). Unlike 2-dimensional echocardiography (2DE), M-mode does not provide a true picture of the heart but rather a diagrammatic display showing changes in the position of structures during the cardiac cycle. Recordings were made initially on hard paper strips, or as Polaroid stop-frame snapshots.

In 1972, 2 HCM cohorts imaged with new M-mode technology were published in *Circulation* 3 months apart (one from the University of California at Los Angeles [22] and one from the National Institutes of Health [23]), quantitatively measuring LV wall thicknesses for the first time. This research represented a major milestone for HCM, providing the opportunity to achieve a reliable noninvasive diagnosis, while avoiding the risk and inconvenience of cardiac catheterization. In the process, a new era of clinical investigation was created (**Central Illustration**).

The asymmetrically hypertrophied ventricular septum was proposed as a diagnostic hallmark (20,23), and the capability for diagnosing HCM in the absence of a subaortic gradient was a major advance since obstruction was a diagnostic prerequisite in the decade before M-mode (1). This scenario is evident by the names used at that time: IHSS (idiopathic hypertrophic subaortic stenosis) and HOCM (hypertrophic obstructive cardiomyopathy) (24,25).

M-mode echocardiography made it possible to compare thicknesses of small portions of the ventricular septum and the LV free wall, and early National Institutes of Health investigators created the "septal-free wall ratio" (20,23). This ratio is usually abnormal in HCM because the anterior septum and posterior wall are generally the thickest and the thinnest portions of the LV chamber, respectively (**Figure 3**). Ratios ≥1.3 were initially promoted as pathognomonic diagnostic markers for HCM, leading to a brief renaming of the disease as "ASH" (asymmetric septal hypertrophy) (20). Unfortunately, characterizing a complex pathological process solely by using a single disease feature only added confusion, given the many acronyms already in use describing the same disease (24,25). Ultimately, the septal-free wall ratio proved to have low diagnostic specificity (26) and soon became obsolete as a HCM marker.

LV OUTFLOW OBSTRUCTION AND IMAGING. Surgical relief of LV outflow tract obstruction (1,2) began

ABBREVIATIONS AND ACRONYMS

2DE = 2-dimensional echocardiography

CMR = cardiac magnetic resonance

CT = computed tomography

LAMP = lysosome-associated membrane protein

LGE = late gadolinium enhancement

LV = left ventricular

LVH = left ventricular hypertrophy

SAM = systolic anterior motion

JACC: CARDIOVASCULAR IMAGING, VOL. 9, NO. 7, 2016
JULY 2016:858–72

FIGURE 1 Timeline for Advances in HCM Since 1958

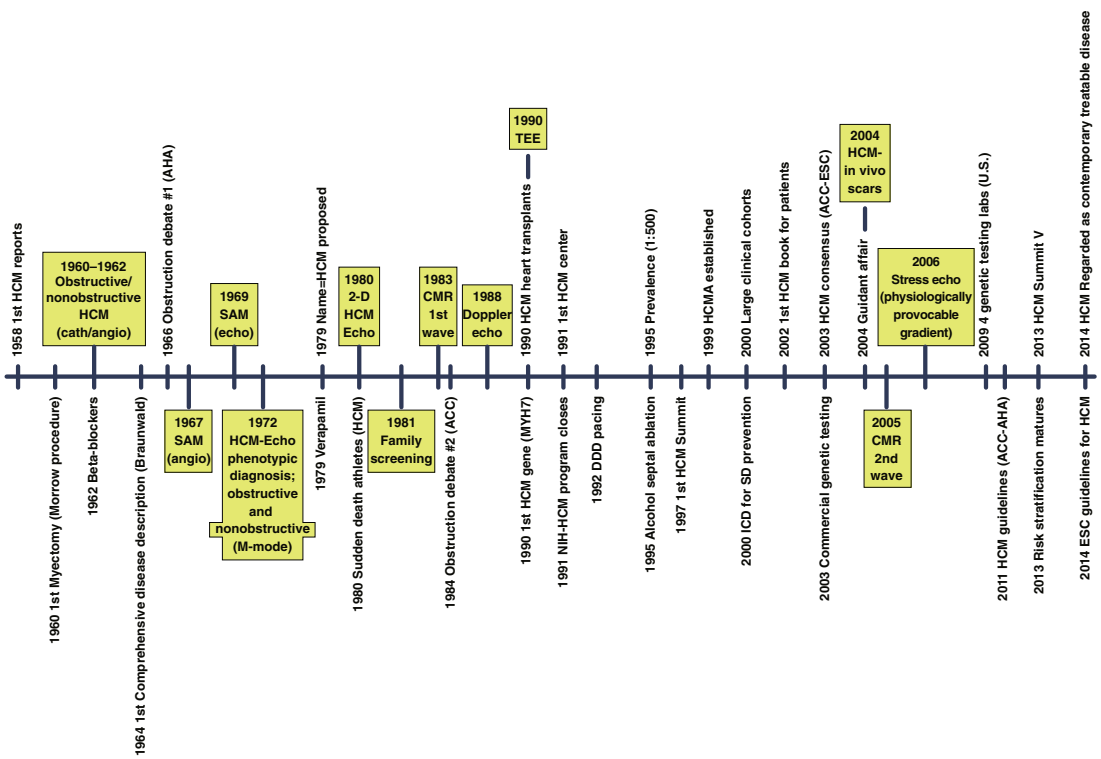

Imaging landmarks are specifically highlighted in **yellow**. 2D = 2-dimensional; ACC = American College of Cardiology; AHA = American Heart Association; angio = angiography; CMR = cardiac magnetic resonance; DDD = dual chamber pacemaker; echo = echocardiography; ESC = European Society of Cardiology; HCM = hypertrophic cardiomyopathy; HCMA = Hypertrophic Cardiomyopathy Association; ICD = implantable cardioverter-defibrillator; MYH7 = beta-myosin heavy chain; NIH = National Institutes of Health; SAM = systolic anterior motion; SD = sudden death; TEE = transesophageal echocardiography.

in the early 1960s (nearly a decade before echocardiography) and progressed at that time even though the true mechanism of subaortic obstruction had not yet been defined. LV outflow tract gradients in HCM were initially attributed to muscular obliteration of the basal outflow tract by the hypertrophied vigorously contracting septum (i.e., "contraction ring"), on the basis of observations made in the operating suite during early septal myectomies (1,27). This concept of obstruction was ultimately supplanted in 1967 by cineangiographers who described the mechanism as mid-systolic contact between the mitral valve and septum, with associated mitral regurgitation (28,29).

In 1969, M-mode echocardiography unequivocally demonstrated that mitral valve systolic anterior motion (SAM) caused subaortic obstruction in HCM (**Figure 4**). This was initially the observation of Dr. Pravin Shah (Rochester, New York), who advanced the use of the acronym "SAM" (30). Thereafter, Popp and Harrison (3) showed that SAM could be provoked with amyl nitrite and abolished with beta-blockers, and Pridie and Oakley (31) reported an "abnormal systolic opening motion of the mitral valve" to cause outflow gradients. Notably, early M-mode studies focused on mitral valve dynamics, with the assessment of hypertrophy evolving 2 to 3 years later as image quality improved.

M-mode also permitted noninvasive estimation of the magnitude of LV outflow obstruction. Investigators, including Dr. Douglas Wigle (Toronto, Ontario, Canada) (32-35), showed that magnitude of the LV outflow gradient was directly related to the duration of systolic contact between the mitral valve and septum, with a quantitative index proposed for estimating gradients (**Figure 4**) (33). Early on, echocardiographic imaging demonstrated that SAM (3,6,30) is abolished by myectomy (34); later, other clinical and imaging observations substantiated that outflow obstruction in HCM is of pathophysiological

FIGURE 2 Imaging Hallmarks for HCM With Respect to M-Mode, 2DE/Doppler, and CMR

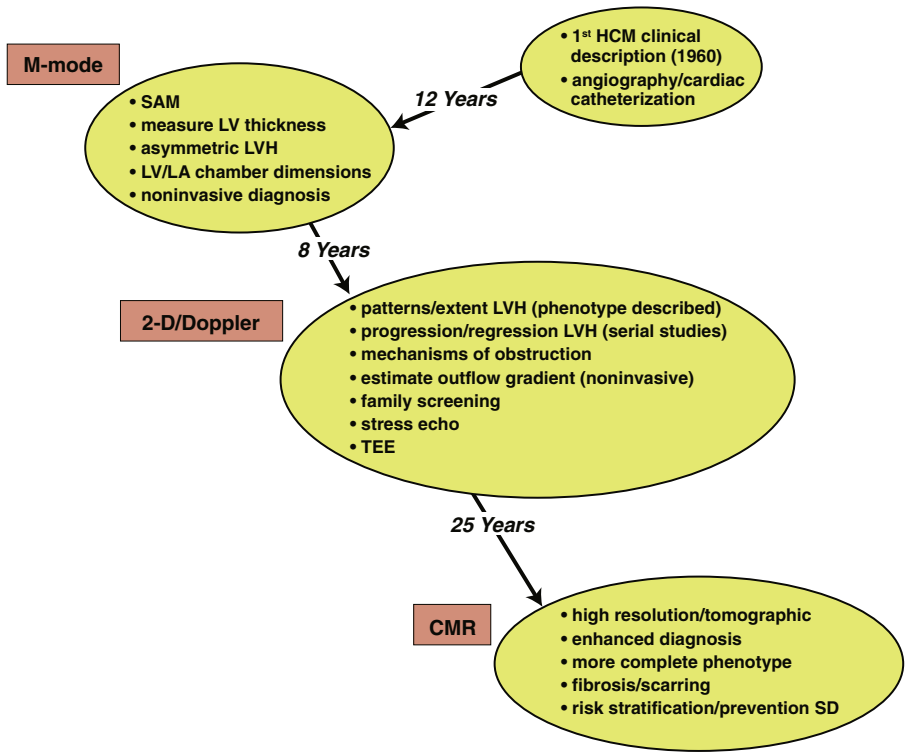

2DE = 2-dimensional echocardiography; LA = left atrial; LV = left ventricular; LVH = left ventricular hypertrophy; other abbreviations as in Figure 1.

significance and represents true impedance to LV outflow (2,36–38). Finally, outcome studies in obstructive HCM negated the now obsolete argument (originally based largely on angiography) that dynamic obstruction in HCM is of no clinical significance (36,37).

Subsequently, impedance to LV outflow was demonstrated with a drop in LV ejection velocities and flow, as well as reduced LV myocardial contraction velocities, all reversible after relief of outflow obstruction by myectomy (2,39–45). Echocardiographic imaging also showed that the dominant hydrodynamic force acting on the mitral valve is drag, the pushing force of flow (rather than Venturi forces) (39–45). Notably, this understanding has contributed to an evolution of the myectomy operation from the classic Morrow procedure (27,36) to the more extended myectomy (46,47). M-mode recordings derived from 2DE images are still used for measurement of chamber dimensions, as well as timing of SAM, due to its target sensitivity and high effective sampling rate.

2-dimensional imaging. Development of cross-sectional cine-imaging scanning dates to 1967, even before M-mode echocardiography (48–52). About 10 years after M-mode was introduced into cardiovascular practice, 2DE imaging became commercially available, first with mechanical sector scanners and then phased array technology providing "wide-angle" real-time images (53). This development expanded visualization of cardiac anatomy in contrast to the static pictures produced by single-dimensional M-mode (Figure 3), constituting another imaging paradigm for clinical researchers and practicing cardiologists. Early real-time 2DE images were considered striking when introduced but required accompanying artistic drawings for publication (Central Illustration); in retrospect, they are many generations in technology removed from present quality and resolution (4,53,54) (Central Illustration, Figures 1, 5, and 6).

2DE studies in HCM initially targeted SAM, subaortic obstruction, and mitral valve motion rather than LVH (53,55). A large 2DE analysis of 125 patients provided the first comprehensive quantitative characterization

JACC: CARDIOVASCULAR IMAGING, VOL. 9, NO. 7, 2016
JULY 2016:858–72

CENTRAL ILLUSTRATION **Evolution in HCM Imaging Over 50 Years**

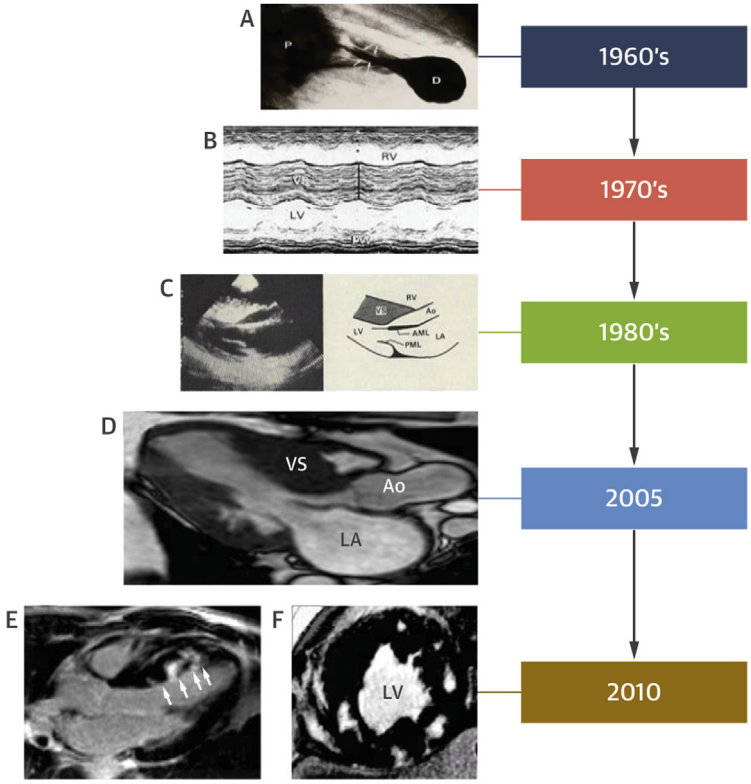

Maron, B.J. et al. J Am Coll Cardiol Img. 2016;9(7):858–72.

(A) Angiogram of the left ventricle (LV) representative of the early 1960s showing mid-ventricular obstruction **(arrows)**. **(B)** M-mode from 1970s showing a disproportionately thickened ventricular septum (VS) compared with a normal posterior wall (PW) thickness. **(C)** 2DE long-axis showing distally hypertrophied VS. **(C)** At the time, an accompanying drawing was usually required for publication. Reprinted with permission from Maron et al. (4). **(D)** CMR image of VS hypertrophy. **(E)** Contrast-enhanced CMR with extensive transmural late gadolinium enhancement (myocardial fibrosis) in VS **(arrows)** of a young, high-risk patient. Reprinted with permission from Maron et al. (124). **(F)** Short-axis CMR showing diffuse multiple focal areas of late gadolinium enhancement in the LV. AML = anterior mitral valve leaflet; Ao = aorta; CMR = cardiac magnetic resonance; HCM = hypertrophic cardiomyopathy; LA = left atrium; PML = posterior mitral valve leaflet; RV = right ventricle; 2DE = 2-dimensional echocardiography.

of the many LVH patterns within the broad HCM disease spectrum (4), followed by an expanded analysis of 600 patients (56). This research created an appreciation for HCM phenotypic heterogeneity and a morphologic classification (4) that is still used (57). Specifically, the continuous short-axis scan showed that although LVH is often distributed diffusely, it may also reside segmentally in isolated sites remote from the anterior septum (4,5,56) (**Figure 3**), as first underscored in a 1981 2DE paper describing "unusual locations of LVH undetected by M-mode" (e.g., posterior septum, anterolateral free wall, and apex [54]).

2DE imaging clarified the diverse mechanisms and clinical implications of LV outflow gradients (58–64) (**Figure 5**); these included patterns of SAM and obstruction by the posterior mitral leaflet (60) or anomalous insertion of papillary muscle into the mitral valve (61), the importance of basal LV outflow tract area (64), as well as the septal anatomy post-muscular resection. With improved image resolution in the 1990s, a number of reliable quantitative observations were possible, including the linear relation between sudden death and LV thickness, and ≥30 mm as an independent sudden death risk marker (65).

Serial echocardiographic studies performed over extended periods of time established important principles; these included phenotype remodeling with increased LV thickness and mass, usually associated with growth during adolescence, but

FIGURE 3 Limitation of "Ice Pick" M-Mode Characterization of LVH (1970s) in HCM

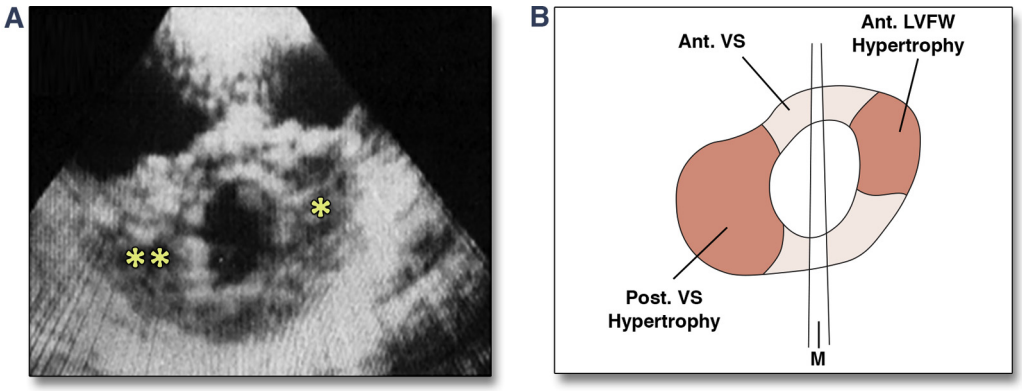

(A) Diagnostic 2DE shows noncontiguous areas of hypertrophy in the posterior septum **(**)** and anterolateral LV **(*)** separated by the anterior septum and posterior free wall of normal thickness. **(B)** Corresponding diagram shows that the dedicated M-mode beam (M) is limited to segments of normal thickness and thereby would fail to image areas of hypertrophy in posterior septum and anterolateral free wall, the septal-free wall ratio would be 1.0 and nondiagnostic (i.e., a false-negative finding) of HCM. From Maron et al. (54). LVFW = left ventricular free wall; LVH = left ventricular hypertrophy; other abbreviations as in Figures 1 and 2.

occasionally in adulthood (66,67). With 2DE visualization of the LV chamber, family screening became far more reliable than was possible with M-mode alone using the septal-free wall ratio (68).

DOPPLER IMAGING. From 1988, Doppler imaging with color flow imaging provided the opportunity to noninvasively estimate LV outflow tract gradients (using the Bernoulli equation) and the magnitude of mitral regurgitation. In 2 studies, Doppler-derived gradients were equivalent to those measured invasively (69,70), altering the long-standing practice of subjecting patients with HCM to serial cardiac catheterizations. Combining continuous wave Doppler imaging with treadmill (stress) exercise testing provided important insights into the clinical course and management of HCM (**Figure 6**) (71). Patients with severe drug-refractory symptoms due to physiologically provoked (exercise) gradients become candidates for heart failure reversal with myectomy (or selectively alcohol ablation) (2,7,71). With all of these advances in echocardiography emerging in <20 years, an imaging examination for HCM was assembled that within 30 min could comprehensively define LV morphology, physiology, and hemodynamic state.

Transesophageal echocardiography introduced in the early 1990s (72) has contributed to intraoperative imaging during myectomy to assess distribution and extent of septal hypertrophy, adequacy of muscular resection, and reduction in SAM. Hand-held miniaturized 2DE instruments are used in selected clinical settings, including intensive care units, emergency departments, ambulances, and outpatient departments (73).

CMR. The initial wave of CMR imaging emerged from the academic radiology community in 1983 (74,75). Case reports and small patient surveys highlighted the diagnostic potential of this new technology. Initially, a major obstacle was CMR images formatted in cross-sectional planes incompatible with standard 2DE, thereby contributing to initial resistance toward this technology on the part of clinical cardiologists. Remarkably, the second wave of advanced CMR did not become relevant to HCM practice for 25 years (76).

It is now evident that CMR technology is ideally suited to the diverse HCM phenotype, providing images with high spatial and temporal resolution, sharp contrast between myocardial borders and blood pool, and tomographic reconstruction of the heart with nonoblique visualization of all LV segments (**Central Illustration**, **Figures 7 and 8**) (76–85). CMR also harbors distinct advantages over 2DE, not encumbered by limited acoustic windows.

Over a decade of study, application of CMR to large HCM cohorts has enhanced diagnosis and clinical management, including recognition of patients not reliably identifiable with 2DE imaging (5,8,76–88). LV wall thickness measurements by CMR are in some patients more precise than with 2DE imaging (**Figure 7**), including improved recognition of the crista supraventricularis muscle that can overestimate LV wall thickness.

JACC: CARDIOVASCULAR IMAGING, VOL. 9, NO. 7, 2016
JULY 2016:858–72

FIGURE 4 Imaging of Subaortic Obstruction

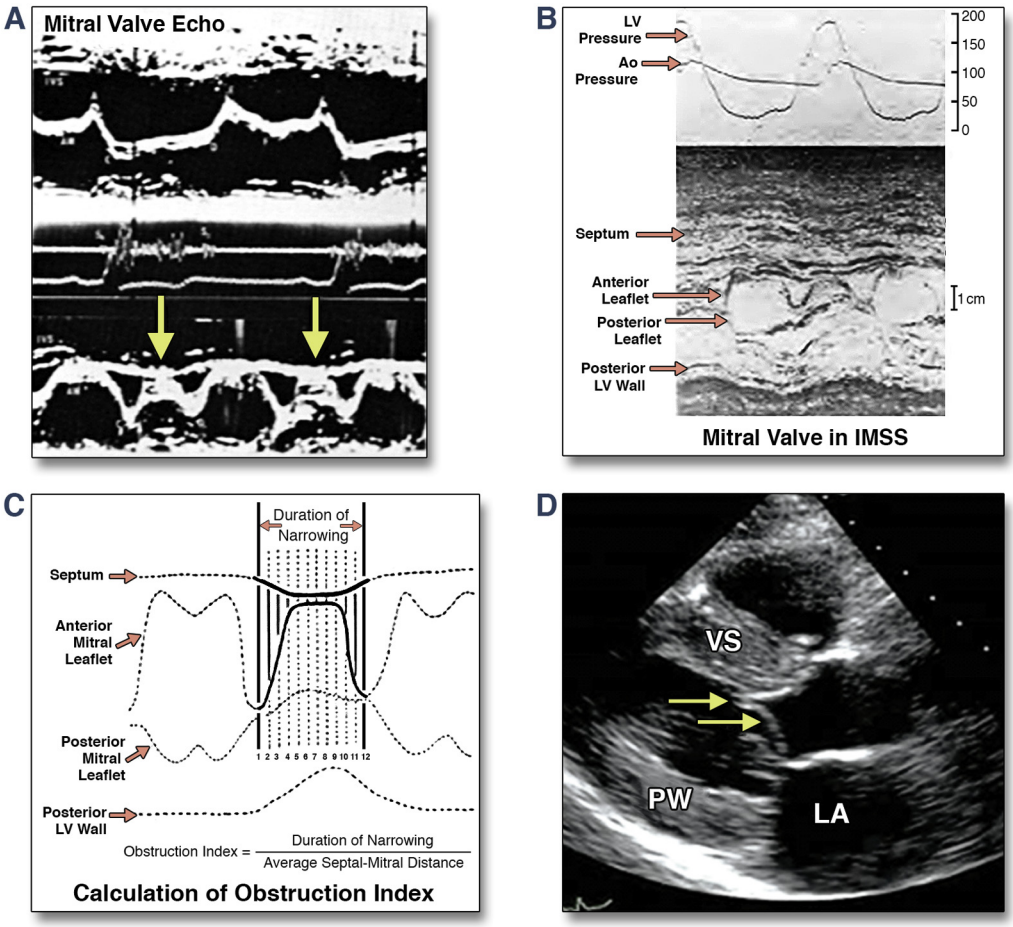

(A to C) M-mode. **(D)** long-axis 2DE. **(A)** 1969: Early M-mode image showing SAM of mitral valve with prolonged septal contact **(arrows)**; reprinted with permission from Shah et al. (30) **(B)** 1970s: SAM and septal contact with simultaneous hemodynamics (marked pressure gradient); reprinted with permission from Henry et al. (33). **(C)** Proposed index to quantitate LV outflow gradient, based on duration of systolic mitral-septal contact; reprinted with permission from Henry et al. (33). **(D)** Elongated anterior mitral leaflet with acute angled bend (SAM) and ventricular septal contact producing outflow obstruction **(arrows)**. LA = left atrium; PW = posterior wall; other abbreviations as in Figures 1 and 2.

Furthermore, just as 2DE imaging revealed large areas of the LV chamber that were not visualized by M-mode, CMR has a similar capability to identify hypertrophied areas "blind" to 2DE imaging, most commonly portions of the most distal (apical) region, posterior septum, and particularly the anterolateral LV free wall for which the epicardial interface can be obscured by pulmonary parenchyma (4,5,8,10,54,76,78,89) (**Figure 8**). *Therefore, as HCM imaging evolved, a consistent principle was that incrementally greater portions of the LV chamber could be more reliably visualized*.

CMR has also expanded the definition of the complex HCM cardiomyopathic process in several respects (**Figure 7**): quantitative assessment of LV mass (not possible reliably with 2DE imaging) (79); extension of hypertrophy into the right ventricular wall (80); noncontiguous segmental hypertrophy (5,8); elongated mitral valve leaflets responsible for outflow obstruction (82); aberrant LV muscle bundles relevant to strategic planning for surgical myectomy (84,85); and de novo onset of LVH in adults (67,86). In addition, CMR was responsible for identifying a new subset of patients; that is, those with LV apical aneurysms and scarring, often associated with mid-cavity muscular obstruction, and with high event rates that may justify the use of primary prevention implantable

FIGURE 5 HCM Phenotype: Evolution of 2DE Image Quality Over 3 Decades

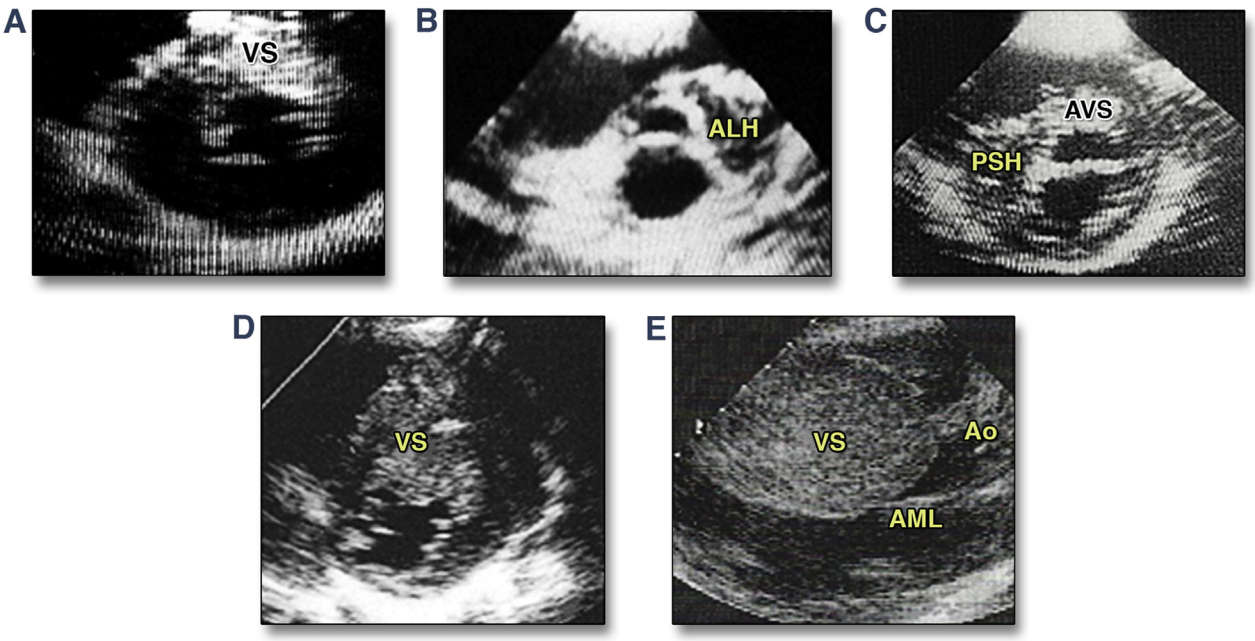

Image from: **(A)** 1979 through to **(E)** the present. Panel **A** is reprinted with permission from Martin et al. (53). ALH = anterolateral hypertrophy; AVS = anterior ventricular septum; PSH = posterior septal hypertrophy; other abbreviations as in Figures 1 and 2.

cardioverter-defibrillators (81,90,91). Some aneurysms (and apical hypertrophy) can also be imaged with the combination of transthoracic echocardiography and the intravenous administration of contrast, effective for LV opacification and defining endocardial borders.

Furthermore, in association with commercial genetic testing, CMR imaging (as well as echocardiography) have been instrumental in defining the novel gene-positive/phenotype-negative subset, by unequivocally demonstrating the absence of LV wall thickening in all segments of the chamber (92).

In addition, early structural and functional markers of affected status have been identified in nonhypertrophied muscle, including diastolic dysfunction, mitral leaflet elongation, myocardial scarring, and narrow blood-filled myocardial crypts (87,88,92,93). Such imaging markers may impact management strategies because the identification of one or more of these structural abnormalities could serve as evidence of positive genetic status in family members in whom genotyping results are negative or ambiguous, or in family members for whom genetic testing has not yet occurred.

Finally, contrast CMR with gadolinium affords the unique capability for in vivo myocardial tissue characterization. In HCM, extensive late gadolinium enhancement (LGE), which is often evidence of myocardial fibrosis and replacement scarring (94-104), is a source of ventricular tachyarrhythmias (104) and an independent prognostic marker for sudden death or appropriate implantable cardioverter-defibrillator discharges (94). LGE ≥15% of LV mass conveys a 2-fold increase in risk and raises consideration for the primary prevention of sudden death with the implantable defibrillator in young patients with, as well as without, other conventional risk markers (94). Absence of LGE is associated with lower risk.

Diffuse transmural high signal intensity LGE is characteristic of end-stage heart failure and systolic dysfunction. Although the initial 2DE description of HCM suggested that multiple speckled echoes ("ground glass texture") in the thickened septum could represent fibrosis (53), contrast CMR showed that this finding is more likely an ultrasound artifact (105).

Contrast CMR has a role in differentiating sarcomeric HCM from phenocopies with LVH. Similar septal and LV free wall thicknesses combined with global subendocardial LGE is highly specific for cardiac amyloidosis (106). Symmetric LVH patterns associated with posterolateral LGE are reported in Fabry disease

JACC: CARDIOVASCULAR IMAGING, VOL. 9, NO. 7, 2016
JULY 2016:858–72

FIGURE 6 Imaging and Clinical Course in HCM

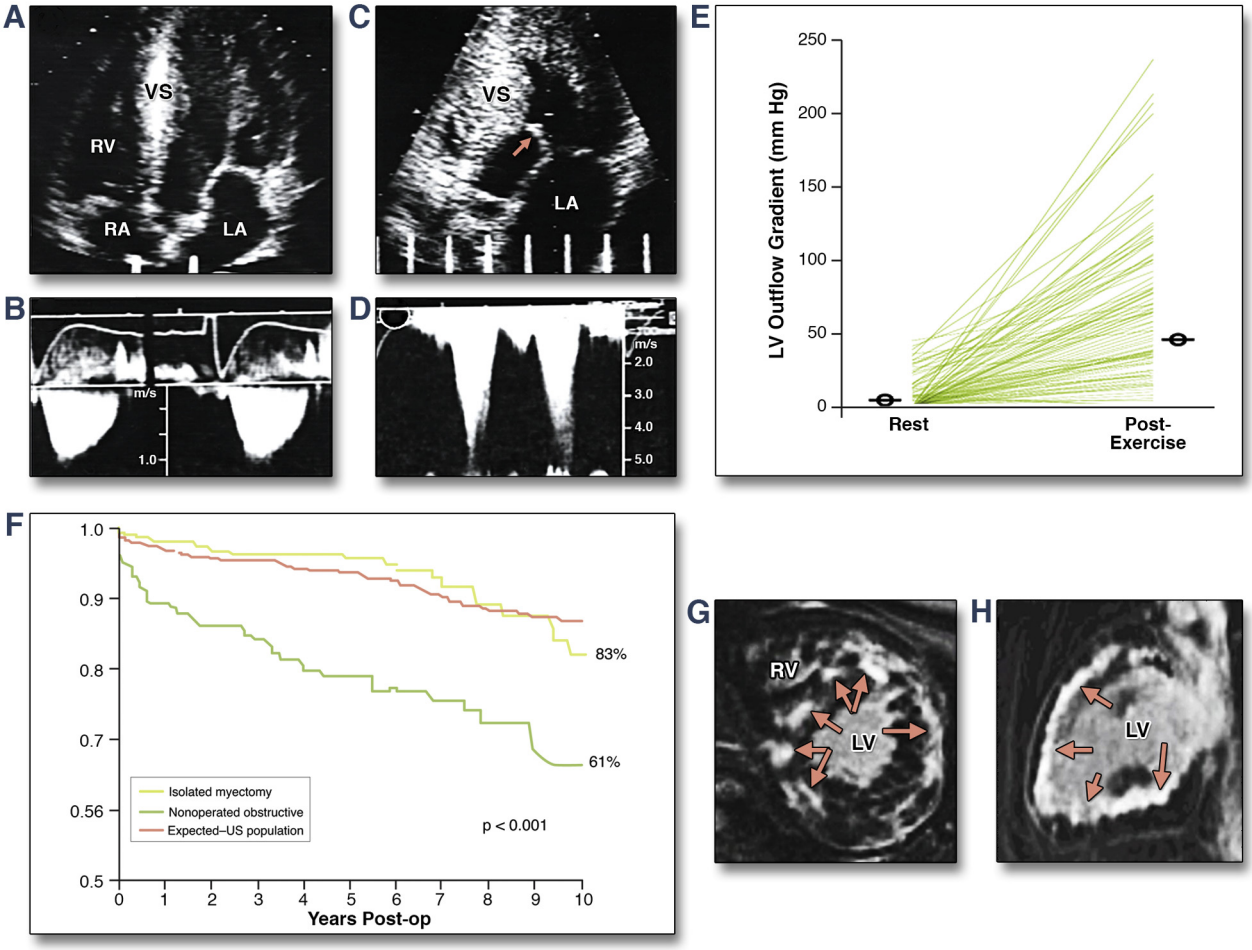

(A) Apical 2DE and **(B)** continuous-wave Doppler showing absence of SAM and obstruction at rest. **(C and D)** Intense exercise provokes SAM-septal contact **(arrow)** and outflow velocity of 5 m/s (100 mm Hg gradient). Reprinted with permission from Maron et al. (71). **(E)** Changes in left ventricular outflow gradient from rest to post-exercise showing physiologically provoked gradients in large consecutive cohort (by mechanism shown in **C and D**). **(F)** Abolition of subaortic gradient by surgical myectomy is associated with long-term (all-cause) survival similar to the general U.S. population. Reprinted with permission from Ommen et al. (125). **(G and H)** End-stage HCM. Two patients with extensive late gadolinium enhancement (myocardial fibrosis) **(arrows)** responsible for systolic dysfunction and progressive heart failure, leading to transplant. RA = right atrium; other abbreviations as in Figures 1 and 2.

(107). Massive LVH and extensive LGE may suggest lysosome-associated membrane protein2 in young patients (108). Distinguishing LV noncompaction from apical HCM can be aided by identifying the deep trabeculations characteristic of noncompaction (109).

OTHER CONSIDERATIONS

Computed tomography (CT) angiography, useful for noninvasively excluding atherosclerotic coronary artery disease in patients with HCM presenting with chest pain, has achieved only selective application for characterizing the HCM phenotype, and is used primarily in those patients ineligible for CMR. Nevertheless, CT imaging possesses superior spatial resolution and may be considered an alternative to CMR for measurement of LV wall thickness and identification of abnormal intraventricular structures.

Positron emission tomography has been periodically promoted in HCM to assess abnormalities of myocardial blood flow due to impaired coronary microvascular function, to determine the etiology of chest pain, or as a marker of increased risk for adverse events (110). However, the limited accessibility of

FIGURE 7 CMR and Diversity of Phenotypic Expression

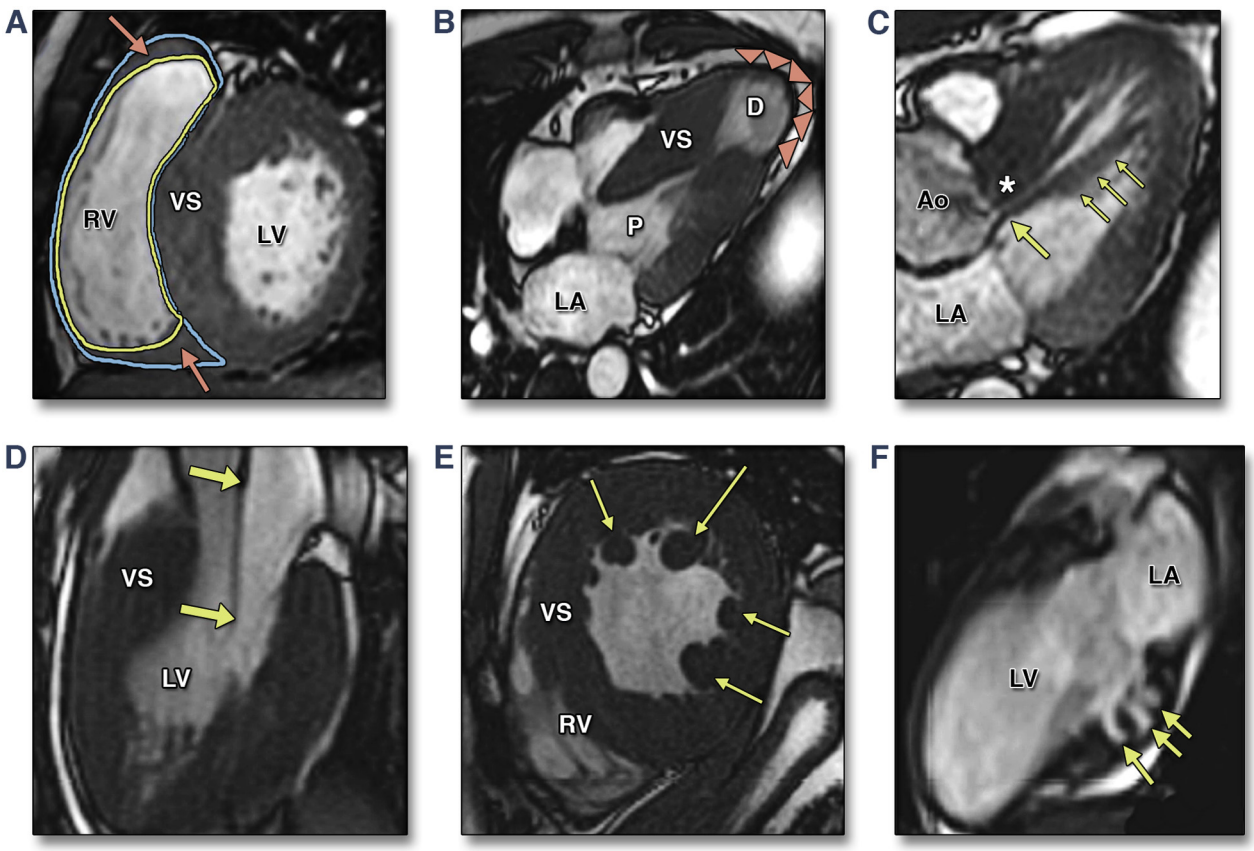

(A) Extension of LVH into RV wall **(arrows)**. From Maron et al. (80). **(B)** Left ventricular apical aneurysm **(arrowheads)** with mid-ventricular obstruction. Reprinted with permission from Maron et al. (81). **(C)** Mid-cavity muscular obstruction. Anomalous direct insertion of anterolateral papillary muscle **(thin arrows)** into anterior mitral leaflet **(thick arrow)** (in the absence of chordae tendineae) making septal contact **(*)**. **(D)** Elongated anterior mitral leaflet **(arrows)**. Reprinted with permission from Maron et al. (82). **(E)** Multiple accessory and hypertrophied papillary muscles which can contribute to outflow obstruction relevant to strategic planning for surgical myectomy **(arrows)**. From Harrigan et al. (84). **(F)** Deep myocardial crypts in posterobasal left ventricular wall **(arrows)**, a morphologic marker for genetically affected relatives without LVH. RV = right ventricle; other abbreviations as in Figures 1 and 2.

positron emission tomography for cardiac imaging has made its integration into clinical practice challenging.

Echocardiography has been used extensively in the noninvasive assessment of diastolic function with transmitral or pulmonary venous pulsed Doppler, tissue Doppler imaging, and (more recently) longitudinal and radial systolic strain imaging and speckle tracking (111–118). These techniques have been of considerable interest for assessing myocardial function, mechanics, and performance, and have provided a variety of insights into HCM disease mechanisms, including: estimation of left-sided filling pressures (111,115), differential diagnoses of physiological versus pathological LVH (112,119), determinants of heart failure (113,120), and diastolic dysfunction preceding LVH in relatives genetically affected with HCM (92,93,116).

Real-time 3-dimensional echocardiography provides a complete cardiac volume rendition with some potential advantages in calculating LV chamber volume and assessing valve structure (121). This technique has been applied to HCM primarily to characterize LV outflow tract anatomy and the mechanism of obstruction. However, the incremental value of 3-dimensional echocardiography over CMR (or 2DE) for clinical management is uncertain, and it remains primarily a research tool.

Genotyping in HCM over the past 30 years has resulted in identification of at least 11 genes encoding proteins of the cardiac sarcomere, and almost 2,000 mutations among these genes, many of which

JACC: CARDIOVASCULAR IMAGING, VOL. 9, NO. 7, 2016
JULY 2016:858–72

FIGURE 8 Advantage of CMR Compared With 2DE

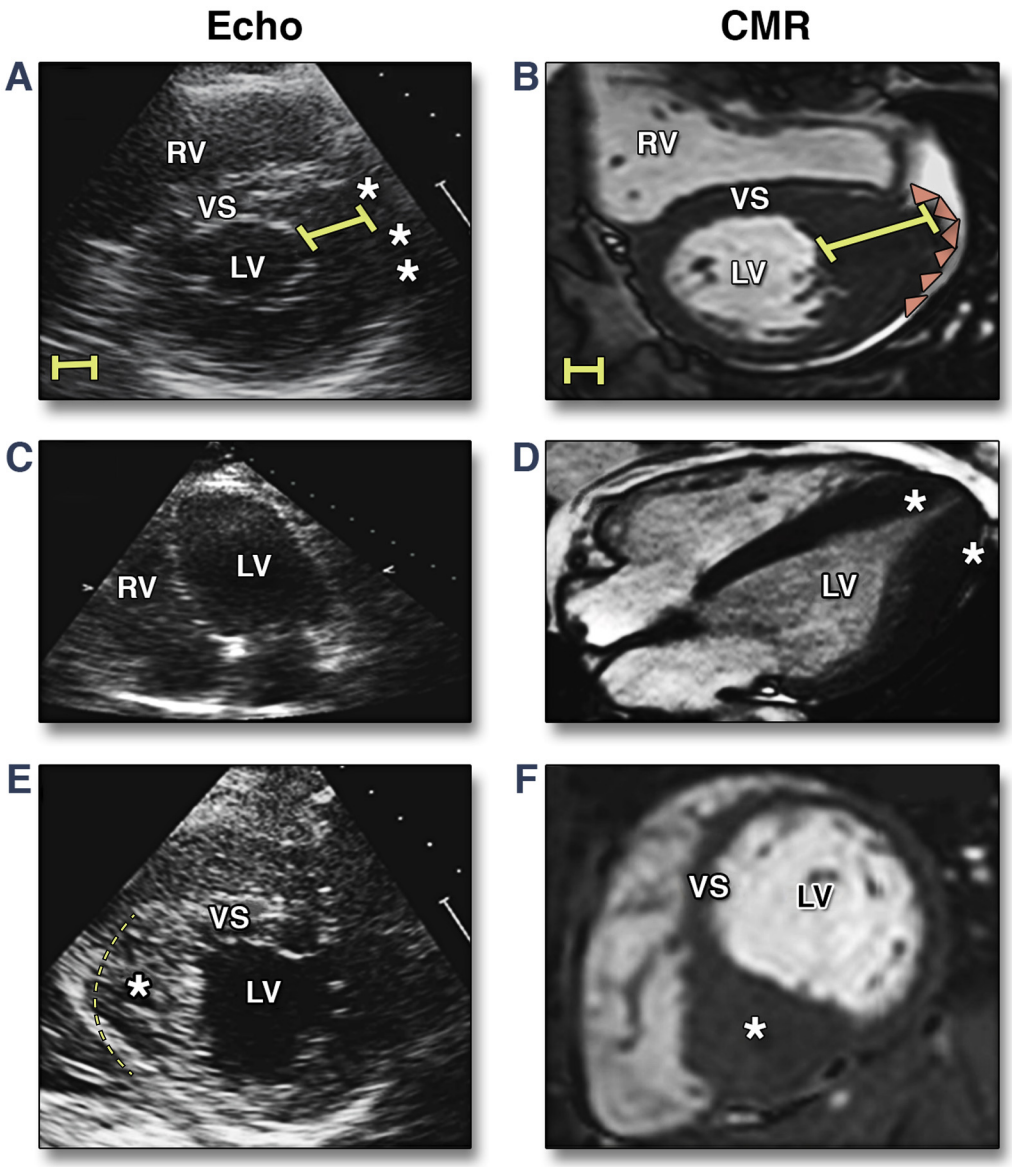

(A) 2DE. Anterolateral LVFW is 18 mm; epicardial border and adjacent extracardiac structures are not well defined **(*)**. **(B)** CMR in the same patient shows well-delineated border of anterolateral LVFW **(arrowheads),** which is massively thickened (35 mm), creating a sudden death risk factor. Reprinted with permission from Maron et al. (78). **(C)** 2DE. Nondiagnostic LV. **(D)** CMR in same patient; shows segmental hypertrophy of left ventricular apex **(*)**, (i.e., apical HCM). Reprinted with permission from Moon et al. (89). **(E)** 2DE. Posterior ventricular septum (VS) thickness is 21 mm **(*)**. **Broken line** denotes endocardial border. **(F)** CMR in same patient; massive hypertrophy (41 mm) **(*)**; creating a sudden death risk marker. Abbreviations as in **Figures 1 to 3**.

are pathogenic for HCM (92). More recently, the MOGE(S) nosology system classification has clarified genotype-phenotype associations by relating imaging-defined cardiac phenotypes (including HCM) to organ(s) involvement, genetic inheritance pattern, etiology/genetic defect, underlying disease/substrate, and functional status (122). However, the enormous diversity in patterns of LVH noted among related family members with HCM, as well as phenotypes as heterogeneous as apical aneurysms, end-stage remodeling, and massive LVH, show that specific genotypes cannot be used to predict clinical phenotypes

(or outcome) in HCM. Conversely, these observations support the notion that HCM is not composed of many unrelated conditions but is rather a unified (albeit diverse) disease of the sarcomere.

FUTURE DIRECTIONS

Due to the remarkable advances in echocardiography and CMR imaging over 5 decades, appreciation for the vast morphologic expression of HCM can be considered highly advanced, at least in terms of clinical diagnosis and investigation. However, the overall HCM imaging story is likely far from over.

We can speculate that the future imaging era for HCM will be focused on emerging techniques defining the myocardial substrate with greater precision, including insights into heart muscle metabolism and biochemistry, as well as more robust tissue characterization, all of which would have been unimaginable to the early pioneers of M-mode and 2DE. For example, CMR-based T_1 mapping is a potential noninvasive imaging marker for the extent of expanded extracellular space within the myocardium (presumably, the combination of interstitial and replacement fibrosis). We expect greater insights into the power of T_1 mapping in HCM with outcome data from the ongoing HCMR (Hypertrophic Cardiomyopathy Registry) study (123).

Such studies will also determine whether T_1 is superior to LGE in differentiating HCM from its phenocopies, including Fabry disease and amyloid or physiological athlete's heart, as well as potentially improving recognition of affected family members at risk for developing HCM with LVH. Incorporating such emerging technology into future clinical trials could possibly determine the efficacy of novel drug or device therapy. T_2-weighted imaging could clarify the clinical significance of edema that may occur as part of the HCM phenotypic expression. Finally, CT scanning with contemporary sequences providing lower radiation exposure, high temporal resolution, and faster acquisition times, as well as its 3-dimensional imaging capability, will have expanded application to HCM.

Incorporating such techniques into clinical studies performed over extended periods of time will also enhance the understanding of phenotypic remodeling and its impact on clinical course. Furthermore, novel contrast agents may emerge capable of differentiating structural components of the myocardium (e.g., interstitial vs. replacement fibrosis). All these advances will contribute clarity to the clinical profile, management, and natural history of patients with HCM.

REPRINT REQUESTS AND CORRESPONDENCE: Dr. Barry J. Maron, HCM Institute, Tufts Medical Center, Division of Cardiology, 800 Washington Street, Box #70, Boston, Massachusetts 02111. E-mail: barrymaron1@gmail.com.

REFERENCES

1. Braunwald E, Lambrew CT, Rockoff SD, Ross J Jr., Morrow AG. Idiopathic hypertrophic subaortic stenosis. I. A description of the disease based upon an analysis of 64 patients. Circulation 1964;30:3–119.

2. Maron BJ, Ommen SR, Semsarian C, et al. Hypertrophic cardiomyopathy: present and future, with translation into contemporary cardiovascular medicine. J Am Coll Cardiol 2014;64:83–99.

3. Popp RL, Harrison DC. Ultrasound in the diagnosis and evaluation of therapy of idiopathic hypertrophic subaortic stenosis. Circulation 1969;40:905–14.

4. Maron BJ, Gottdiener JS, Epstein SE. Patterns and significance of distribution of left ventricular hypertrophy in hypertrophic cardiomyopathy. A wide-angle, two- dimensional echocardiographic study of 125 patients. Am J Cardiol 1981;48:418–28.

5. Maron MS, Maron BJ, Harrigan C, et al. Hypertrophic cardiomyopathy phenotype revisited after 50 years with cardiovascular magnetic resonance. J Am Coll Cardiol 2009;54:220–8.

6. Wigle ED, Sasson Z, Henderson MA, et al. Hypertrophic cardiomyopathy. The importance of the site and the extent of hypertrophy. A review. Prog Cardiovasc Dis 1985;28:1–83.

7. Maron BJ, Maron MS. Hypertrophic cardiomyopathy. Lancet 2013;381:242–55.

8. Maron MS, Maron BJ. Clinical impact of contemporary cardiovascular magnetic resonance imaging in hypertrophic cardiomyopathy. Circulation 2015;132:292–8.

9. Tajik AJ, Giuliani ER. Echocardiographic observations in idiopathic hypertrophic subaortic stenosis. Mayo Clin Proc 1974;49:89–97.

10. Nagueh SF, Bierig SM, Budoff MJ, et al. American Society of Echocardiography clinical recommendations for multimodality cardiovascular imaging of patients with hypertrophic cardiomyopathy: endorsed by the American Society of Nuclear Cardiology, Society for Cardiovascular Magnetic Resonance, and Society of Cardiovascular Computed Tomography. J Am Soc Echocardiogr 2011;24:473–98.

11. Feigenbaum H. Clinical applications of echocardiography. Prog Cardiovasc Dis 1972;14:531–58.

12. Feigenbaum H, Popp RL, Chip JN, Haine CL. Left ventricular wall thickness measured by ultrasound. Arch Intern Med 1968;121:391–5.

13. Feigenbaum H, Waldhausen JA, Hyde LP. Ultrasound diagnosis of pericardial effusion. JAMA 1965;191:711–4.

14. Popp RL, Wolfe SB, Hirata T, Feigenbaum H. Estimation of right and left ventricular size by ultrasound. A study of the echoes from the interventricular septum. Am J Cardiol 1969;24:523–30.

15. Feigenbaum H, Popp RL, Wolfe SB, et al. Ultrasound measurements of the left ventricle. A correlative study with angiocardiography. Arch Intern Med 1972;129:461–7.

16. Hirata T, Wolfe SB, Popp RL, Helmen CH, Feigenbaum H. Estimation of left atrial size using ultrasound. Am Heart J 1969;78:43–52.

17. Joyner CR, Reid JM, Bond JP. Reflected ultrasound in the assessment of mitral valve disease. Circulation 1963;27:503–11.

18. Gramiak R, Shah PM. Echocardiography of the normal and diseased aortic valve. Radiology 1970;107:175–80.

19. Teare D. Asymmetrical hypertrophy of the heart in young adults. Br Heart J 1958;20:1–8.

20. Henry WL, Clark CE, Epstein SE. Asymmetric septal hypertrophy (ASH): the unifying link in the IHSS disease spectrum. Observations regarding its

pathogenesis, pathophysiology, and course. Circulation 1973;47:827–32.

21. Maron BJ, Bonow RO, Salberg L, Roberts WC, Braunwald E. The first patient clinically diagnosed with hypertrophic cardiomyopathy. Am J Cardiol 2008;102:1418–20.

22. Abbasi AS, MacAlpin RN, Eber LM, Pearce ML. Echocardiographic diagnosis of idiopathic hypertrophic cardiomyopathy without outflow obstruction. Circulation 1972;46:897–904.

23. Henry WL, Clark CE, Epstein SE. Asymmetric septal hypertrophy. Echocardiographic identification of the pathognomonic anatomic abnormality of IHSS. Circulation 1973;47:225–33.

24. Maron BJ, Epstein SE. Hypertrophic cardiomyopathy: a discussion of nomenclature. Am J Cardiol 1979;43:1242–4.

25. Maron BJ, Seidman CE, Ackerman MJ, et al. How should hypertrophic cardiomyopathy be classified? What's in a name? Dilemmas in nomenclature characterizing hypertrophic cardiomyopathy and left ventricular hypertrophy. Circ Cardiovasc Genet 2009;2:81–5.

26. Maron BJ, Clark CE, Henry WL, et al. Prevalence and characteristics of disproportionate ventricular septal thickening in patients with acquired or congenital heart diseases: echocardiographic and morphologic findings. Circulation 1977;55:489–96.

27. Maron BJ, Braunwald E. Eugene Braunwald, MD and the early years of hypertrophic cardiomyopathy: a conversation with Dr. Barry J. Maron. Am J Cardiol 2012;109:1539–47.

28. Simon AL, Ross J Jr., Gault JH. Angiographic anatomy of the left ventricle and mitral valve in idiopathic hypertrophic subaortic stenosis. Circulation 1967;36:852–67.

29. Fix P, Moberg A, Soederberg H, Karnell J. Muscular subvalvular aortic stenosis; abnormal anterior mitral leaflet possibly the primary factor. Acta Radiol Diagn (Stockh) 1964;2:177–93.

30. Shah PM, Gramiak R, Kramer DH. Ultrasound localization of left ventricular outflow obstruction in hypertrophic obstructive cardiomyopathy. Circulation 1969;40:3–11.

31. Pridie RB, Oakley CM. Mechanism of mitral regurgitation in hypertrophic obstructive cardiomyopathy. Br Heart J 1970;32:203–8.

32. Pollick C, Rakowski H, Wigle ED. Muscular subaortic stenosis: the quantitative relationship between systolic anterior motion and the pressure gradient. Circulation 1984;69:43–9.

33. Henry WL, Clark CE, Glancy DL, Epstein SE. Echocardiographic measurement of the left ventricular outflow gradient in idiopathic hypertrophic subaortic stenosis. N Engl J Med 1973;288:989–93.

34. Shah PM, Gramiak R, Adelman AG, Wigle ED. Role of echocardiography in diagnostic and hemodynamic assessment of hypertrophic subaortic stenosis. Circulation 1971;44:891–8.

35. Pollick C, Morgan CD, Gilbert BW, Rakowski H, Wigle ED. Muscular subaortic stenosis: the temporal relationship between systolic anterior motion of the anterior mitral leaflet and the pressure gradient. Circulation 1982;66:1087–94.

36. Maron BJ, Maron MS, Wigle ED, Braunwald E. The 50-year history, controversy, and clinical implications of left ventricular outflow tract obstruction in hypertrophic cardiomyopathy from idiopathic hypertrophic subaortic stenosis to hypertrophic cardiomyopathy. J Am Coll Cardiol 2009;54:191–200.

37. Maron MS, Olivotto I, Betocchi S, et al. Effect of left ventricular outflow tract obstruction on clinical outcome in hypertrophic cardiomyopathy. N Engl J Med 2003;348:295–303.

38. Maron BJ, Gottdiener JS, Arce J, Rosing DR, Wesley YE, Epstein SE. Dynamic subaortic obstruction in hypertrophic cardiomyopathy: analysis by pulsed Doppler echocardiography. J Am Coll Cardiol 1985;6:1–18.

39. Sherrid MV, Gunsburg DZ, Pearle G. Mid-systolic drop in ventricular ejection velocity in obstructive hypertrophic cardiomyopathy—the lobster claw abnormality. J Am Soc Echocardiogr 1997;10:707–12.

40. Breithardt OA, Beer G, Stolle B, et al. Mid systolic septal deceleration in hypertrophic cardiomyopathy: clinical value and insights into the pathophysiology of outflow tract obstruction by tissue Doppler echocardiography. Heart 2005;91:379–80.

41. Conklin HM, Huang X, Davies CH, Sahn DJ, Shively BK. Biphasic left ventricular outflow and its mechanism in hypertrophic obstructive cardiomyopathy. J Am Soc Echocardiogr 2004;17:375–83.

42. Barac I, Upadya S, Pilchik R, et al. Effect of obstruction on longitudinal left ventricular shortening in hypertrophic cardiomyopathy. J Am Coll Cardiol 2007;49:1203–11.

43. Sherrid MV, Wever-Pinzon O, Shah A, Chaudhry FA. Reflections of inflections in hypertrophic cardiomyopathy. J Am Coll Cardiol 2009;54:212–9.

44. Jiang L, Levine RA, King ME, Weyman AE. An integrated mechanism for systolic anterior motion of the mitral valve in hypertrophic cardiomyopathy based on echocardiographic observations. Am Heart J 1987;113:633–44.

45. Ro R, Halpern D, Sahn DJ, et al. Vector flow mapping in obstructive hypertrophic cardiomyopathy to assess the relationship of early systolic left ventricular flow and the mitral valve. J Am Coll Cardiol 2014;64:1984–95.

46. Messmer BJ. Extended myectomy for hypertrophic obstructive cardiomyopathy. Ann Thorac Surg 1994;58:575–7.

47. Sherrid M, Chaudhry FA, Swistel DG. Obstructive hypertrophic cardiomyopathy. Echocardiography, pathophysiology, and the continuing evolution of surgery for obstruction. Ann Thorac Surg 2003;75:620–32.

48. Ebina T, Oka S, Tanaka M, Kosaka S, Terasawa Y. The ultrasono-tomography for the heart and great vessels in living human subjects by means of the ultrasonic reflection technique. Jpn Heart J 1967;8:331–53.

49. Bom N, Lancee CT, van Zwieten G, Kloster FE, Roelandt J. Multiscan echocardiography. I. Technical description. Circulation 1973;48:1066–74.

50. Griffith JM, Henry WL. A sector scanner for real time two-dimensional echocardiography. Circulation 1974;49:1147–52.

51. Gramiak R, Waag RC, Simon W. Cine ultrasound cardiography. Radiology 1973;107:175–80.

52. King DL. Cardiac ultrasonography. Cross-sectional ultrasonic imaging of the heart. Circulation 1973;47:843–7.

53. Martin RP, Rakowski H, French J, Popp RL. Idiopathic hypertrophic subaortic stenosis viewed by wide-angle, phased-array echocardiography. Circulation 1979;59:1206–17.

54. Maron BJ, Gottdiener JS, Bonow RO, Epstein SE. Hypertrophic cardiomyopathy with unusual locations of left ventricular hypertrophy undetectable by M-mode echocardiography. Identification by wide-angle two-dimensional echocardiography. Circulation 1981;63:409–18.

55. Rossen RM, Goodman DJ, Ingham RE, Popp RL. Echocardiographic criteria in the diagnosis of idiopathic hypertrophic subaortic stenosis. Circulation 1974;50:747–51.

56. Klues HG, Schiffers A, Maron BJ. Phenotypic spectrum and patterns of left ventricular hypertrophy in hypertrophic cardiomyopathy: morphologic observations and significance as assessed by two-dimensional echocardiography in 600 patients. J Am Coll Cardiol 1995;26:1699–708.

57. Reant P, Donal E, Schnell F, et al. Clinical and imaging description of the Maron subtypes of hypertrophic cardiomyopathy. Int J Cardiovasc Imaging 2015;31:47–55.

58. Shah PM, Taylor RD, Wong M. Abnormal mitral valve coaptation in hypertrophic obstructive cardiomyopathy: proposed role in systolic anterior motion of mitral valve. Am J Cardiol 1982;48:258–62.

59. Spirito P, Maron BJ. Patterns of systolic anterior motion of the mitral valve in hypertrophic cardiomyopathy: assessment by two-dimensional echocardiography. Am J Cardiol 1984;54:1039–46.

60. Maron BJ, Harding AM, Spirito P, Roberts WC, Waller BF. Systolic anterior motion of the posterior mitral leaflet: a previously unrecognized cause of dynamic subaortic obstruction in patients with hypertrophic cardiomyopathy. Circulation 1983;68:282–93.

61. Klues HG, Roberts WC, Maron BJ. Anomalous insertion of papillary muscle directly into anterior mitral leaflet in hypertrophic cardiomyopathy. Significance in producing left ventricular outflow obstruction. Circulation 1991;84:1188–97.

62. Sherrid MV, Gunsburg DZ, Modenhauer S, Pearle G. Systolic anterior motion begins at low left ventricular outflow tract velocity in obstructive hypertrophic cardiomyopathy. J Am Coll Cardiol 2000;36:1344–54.

63. Klues HG, Roberts WC, Maron BJ. Morphological determinants of echocardiographic patterns of mitral valve systolic anterior motion in obstructive hypertrophic cardiomyopathy. Circulation 1993;87:1570–9.

64. Spirito P, Maron BJ. Significance of left ventricular outflow tract cross-sectional area in hypertrophic cardiomyopathy: a two-dimensional

echocardiographic assessment. Circulation 1983;67:1100–8.

65. Spirito P, Bellone P, Harris KM, Bernabo P, Bruzzi P, Maron BJ. Magnitude of left ventricular hypertrophy and risk of sudden death in hypertrophic cardiomyopathy. N Engl J Med 2000;342:1778–85.

66. Maron BJ, Spirito P, Wesley Y, Arce J. Development and progression of left ventricular hypertrophy in children with hypertrophic cardiomyopathy. N Engl J Med 1986;315:610–4.

67. Maron BJ, Niimura H, Casey SA, et al. Development of left ventricular hypertrophy in adults in hypertrophic cardiomyopathy caused by cardiac myosin-binding protein C gene mutations. J Am Coll Cardiol 2001;38:315–21.

68. Maron BJ, Nichols PF III, Pickle LW, Wesley YE, Mulvihill JJ. Patterns of inheritance in hypertrophic cardiomyopathy: assessment by M-mode and two-dimensional echocardiography. Am J Cardiol 1984;53:1087–94.

69. Sasson Z, Yock PG, Hatle LK, Alderman EL, Popp RL. Doppler echocardiographic determination of the pressure gradient in hypertrophic cardiomyopathy. J Am Coll Cardiol 1988;11:752–6.

70. Panza JA, Petrone RK, Fananapazir L, Maron BJ. Utility of continuous wave Doppler echocardiography in the noninvasive assessment of left ventricular outflow tract pressure gradient in patients with hypertrophic cardiomyopathy. J Am Coll Cardiol 1992;19:91–9.

71. Maron MS, Olivotto I, Zenovich AG, et al. Hypertrophic cardiomyopathy is predominantly a disease of left ventricular outflow tract obstruction. Circulation 2006;114:2232–9.

72. Grigg LE, Wigle ED, Williams WG, Daniel LB, Rakowski H. Transesophageal Doppler echocardiography in obstructive hypertrophic cardiomyopathy: clarification of pathophysiology and importance in intraoperative decision making. J Am Coll Cardiol 1992;20:42–52.

73. Sicari R, Galderisi M, Voigt JU, et al. The use of pocket-size imaging devices: a position statement of the European Association of Echocardiography. Eur J Echocardiogr 2011;12:85–7.

74. Higgins CB. Overview of MR of the heart—1986. Am J Roentgenol 1986;146:907–18.

75. Higgins CB, Byrd BF 3rd, Stark D, et al. Magnetic resonance imaging in hypertrophic cardiomyopathy. Am J Cardiol 1985;55:1121–6.

76. Rickers C, Wilke NM, Jerosch-Herold M, et al. Utility of cardiac magnetic resonance imaging in the diagnosis of hypertrophic cardiomyopathy. Circulation 2005;112:855–61.

77. Cannavale A, Ordovas KG, Higgins CB. Magnetic resonance imaging of hypertrophic cardiomyopathy. J Thorac Imaging 2013;28:W12–8.

78. Maron MS, Lesser JR, Maron BJ. Management implications of massive left ventricular hypertrophy in hypertrophic cardiomyopathy significantly underestimated by echocardiography but identified by cardiovascular magnetic resonance. Am J Cardiol 2010;105:1842–3.

79. Olivotto I, Maron MS, Autore C, et al. Assessment and significance of left ventricular mass by cardiovascular magnetic resonance in hypertrophic cardiomyopathy. J Am Coll Cardiol 2008;52:559–66.

80. Maron MS, Hauser TH, Dubrow E, et al. Right ventricular involvement in hypertrophic cardiomyopathy. Am J Cardiol 2007;100:1293–8.

81. Maron MS, Finley JJ, Bos JM, et al. Prevalence, clinical significance, and natural history of left ventricular apical aneurysms in hypertrophic cardiomyopathy. Circulation 2008;118:1541–9.

82. Maron MS, Olivotto I, Harrigan C, et al. Mitral valve abnormalities identified by cardiovascular magnetic resonance represent a primary phenotypic expression of hypertrophic cardiomyopathy. Circulation 2011;124:40–7.

83. Nagata Y, Konno T, Fujino N, et al. Right ventricular hypertrophy is associated with cardiovascular events in hypertrophic cardiomyopathy: evidence from study with magnetic resonance imaging. Can J Cardiol 2015;31:702–8.

84. Harrigan CJ, Appelbaum E, Maron BJ, et al. Significance of papillary muscle abnormalities identified by cardiovascular magnetic resonance in hypertrophic cardiomyopathy. Am J Cardiol 2008;101:668–73.

85. Gruner C, Chan RH, Crean A, et al. Significance of left ventricular apical-basal muscle bundle identified by cardiovascular magnetic resonance imaging in patients with hypertrophic cardiomyopathy. Eur Heart J 2014;35:2706–13.

86. Maron BJ, Haas TS, Kitner C, Lesser JR. Onset of apical hypertrophic cardiomyopathy in adulthood. Am J Cardiol 2011;108:1783–7.

87. Maron MS, Rowin EJ, Lin D, et al. Prevalence and clinical profile of myocardial crypts in hypertrophic cardiomyopathy. Circ Cardiovasc Imaging 2012;5:441–7.

88. Captur G, Lopes LR, Mohun TJ, et al. Prediction of sarcomere mutations in subclinical hypertrophic cardiomyopathy. Circ Cardiovasc Imaging 2014;7:863–71.

89. Moon JC, Fisher NG, McKenna WJ, Pennell DJ. Detection of apical hypertrophic cardiomyopathy by cardiovascular magnetic resonance in patients with non-diagnostic echocardiography. Heart 2004;90:645–90.

90. Nakamura T, Matsubarra K, Furukawa K, et al. Diastolic paradox jet flow in patients with hypertrophic cardiomyopathy: evidence of concealed apical asynergy with cavity obliteration. J Am Coll Cardiol 1992;19:516–24.

91. Po JR, Kim B, Aslam F, et al. Doppler systolic signal void in hypertrophic cardiomyopathy: apical aneurysm and severe obstruction without elevated intraventricular velocities. J Am Soc Echocardiogr 2015;28:1462–73.

92. Maron BJ, Maron MS, Semsarian C. Genetics of hypertrophic cardiomyopathy after 20 years: clinical perspectives. J Am Coll Cardiol 2012;60:705–15.

93. Ho CY, Sweitzer NK, McDonough B, et al. Assessment of diastolic function with Doppler tissue imaging to predict genotype in preclinical hypertrophic cardiomyopathy. Circulation 2002;105:2292–7.

94. Chan RH, Maron BJ, Olivotto I, et al. Prognostic value of quantitative contrast-enhanced cardiovascular magnetic resonance for the evaluation of sudden death risk in patients with hypertrophic cardiomyopathy. Circulation 2014;130:484–95.

95. O'Hanlon R, Grasso A, Roughton M, et al. Prognostic significance of myocardial fibrosis in hypertrophic cardiomyopathy. J Am Coll Cardiol 2010;56:867–74.

96. Olivotto I, Maron BJ, Appelbaum E, et al. Spectrum and clinical significance of systolic function and myocardial fibrosis assessed by cardiovascular magnetic resonance in hypertrophic cardiomyopathy. Am J Cardiol 2010;106:261–7.

97. Rubinshtein R, Glockner JF, Ommen SR, et al. Characteristics and clinical significance of late gadolinium enhancement by contrast-enhanced magnetic resonance imaging in patients with hypertrophic cardiomyopathy. Circ Heart Fail 2010;3:51–8.

98. Bruder O, Wagner A, Jensen CJ, et al. Myocardial scar visualized by cardiovascular magnetic resonance imaging predicts major adverse events in patients with hypertrophic cardiomyopathy. J Am Coll Cardiol 2010;56:875–87.

99. Smith BM, Dorfman AL, Yu S, et al. Clinical significance of late gadolinium enhancement in patients <20 years of age with hypertrophic cardiomyopathy. J Am J Cardiol 2014;113:1234–9.

100. van Dockum WG, ten Cate FJ, ten Berg JM, et al. Myocardial infarction after percutaneous transluminal septal myocardial ablation in hypertrophic obstructive cardiomyopathy: evaluation by contrast-enhanced magnetic resonance imaging. J Am Coll Cardiol 2004;43:27–34.

101. Valeti US, Nishimura RA, Holmes DR, et al. Comparison of surgical septal myectomy and alcohol septal ablation with cardiac magnetic resonance imaging in patients with hypertrophic obstructive cardiomyopathy. J Am Coll Cardiol 2007;49:350–7.

102. Ismail TF, Jabbour A, Gulati A, et al. Role of late gadolinium enhancement cardiovascular magnetic resonance in the risk stratification of hypertrophic cardiomyopathy. Heart 2014;100:1851–8.

103. Chan RH, Maron BJ, Olivotto I, et al. Significance of late gadolinium enhancement at right ventricular attachment to ventricular septum in patients with hypertrophic cardiomyopathy. Am J Cardiol 2015;116:436–41.

104. Adabag AS, Maron BJ, Appelbaum E, et al. Occurrence and frequency of arrhythmias in hypertrophic cardiomyopathy in relation to delayed enhancement on cardiovascular magnetic resonance. J Am Coll Cardiol 2008;51:1369–74.

105. Maron BJ, Lindberg J, Haas TS, et al. "Speckled" ventricular septum in hypertrophic cardiomyopathy revisited after 30 years. Am J Cardiol 2011;107:1862–3.

106. Austin BA, Tang WH, Rodriquez ER, et al. Delayed hyper-enhancement magnetic resonance imaging provides incremental diagnostic and prognostic utility in suspected cardiac amyloidosis. J Am Coll Cardiol Img 2009;2:1369–77.

107. Moon J, Sachdev B, Elkington AG, et al. Gadolinium enhanced cardiovascular magnetic

resonance in Anderson-Fabry disease. Eur Heart J 2003;24:2151–5.

108. Maron BJ, Roberts WC, Arad M, et al. Clinical outcome and phenotypic expression in LAMP2 cardiomyopathy. JAMA 2009;301:1253–9.

109. Kelley-Hedgepeth A, Towbin JA, Maron MS. Images in cardiovascular medicine. Overlapping phenotypes: left ventricular noncompaction and hypertrophic cardiomyopathy. Circulation 2009; 119:e588–9.

110. Cecchi F, Olivotto I, Gistri R, et al. Coronary microvascular dysfunction and prognosis in hypertrophic cardiomyopathy. N Engl J Med 2003; 349:1027–35.

111. Geske JB, Sorajja P, Nishimura RA, Ommen SR. Evaluation of left ventricular filling pressures by Doppler echocardiography in patients with hypertrophic cardiomyopathy: correlation with direct left atrial pressure measurement at cardiac catheterization. Circulation 2007;116:2702–8.

112. Vinereanu D, Florescu N, Sculthorpe N, et al. Differentiation between pathologic and physiologic left ventricular hypertrophy by tissue Doppler assessment of long-axis function in patients with hypertrophic cardiomyopathy or systemic hypertension and in athletes. Am J Cardiol 2001;88:53–8.

113. Maron BJ, Spirito P, Green KJ, Wesley YE, Bonow RO, Arce J. Noninvasive assessment of left ventricular diastolic function by pulsed Doppler echocardiography in patients with hypertrophic cardiomyopathy. J Am Coll Cardiol 1987;10: 733–42.

114. Carasso S, Yang H, Woo A, et al. Systolic myocardial mechanics in hypertrophic cardiomyopathy: novel concepts and implications for clinical status. J Am Soc Echocardiogr 2008;21: 675–83.

115. Nagueh SF, Lakkis NM, Middleton KJ, Spencer WH III, Zoghbi WA, Quinones MA. Doppler estimation of left ventricular filling pressures in patients with hypertrophic cardiomyopathy. Circulation 1999;99:254–61.

116. Nagueh SF, McFalls J, Meyer D. Tissue Doppler imaging predicts the development of hypertrophic cardiomyopathy in subjects with subclinical disease. Circulation 2003;108:395–8.

117. Nucifora G, Muser D, Gianfagna P, Morocutti G, Proclemer A. Systolic and diastolic myocardial mechanics in hypertrophic cardiomyopathy and their link to the extent of hypertrophy, replacement fibrosis and interstitial fibrosis. Int J Cardiovasc Imaging 2015;31: 1603–10.

118. Ho CY, Carlsen C, Thune JJ, et al. Echocardiographic strain imaging to assess early and late consequences of sarcomere mutations in hypertrophic cardiomyopathy. Circ Cardiovasc Genet 2009;2:314–21.

119. Maron BJ, Nishimura RA, Cooper LT Jr., et al. Eligibility and disqualification recommendations for competitive athletes with cardiovascular abnormalities: Task Force 3: hypertrophic cardiomyopathy, arrhythmogenic right ventricular cardiomyopathy and other cardiomyopathies, and myocarditis. J Am Coll Cardiol 2015;66: 2362–71.

120. Kalra A, Harris KM, Maron BA, et al. Association of Doppler tissue imaging parameters with heart failure progression in hypertrophic cardiomyopathy. Am J Cardiol 2016;117:1808–14.

121. Kuhl HP, Franke A, Janssens U, et al. Three-dimensional echocardiographic determination of left ventricular volumes and function by multiplane transesophageal transducer: dynamic in vitro validation and in vivo comparison with angiography and thermodilution. J Am Soc Echocardiogr 1998;11:1113–24.

122. Arbustini E, Narula N, Tavazzi L, et al. The MOGE(S) classification of cardiomyopathy for clinicians. J Am Coll Cardiol 2014;64:304–18.

123. Kramer CM, Appelbaum E, Desai MY, et al. Hypertrophic Cardiomyopathy Registry: the rationale and design of an international, observational study of hypertrophic cardiomyopathy. Am Heart J 2015;170:223–30.

124. Maron BJ. Contemporary insights and strategies for risk stratification and prevention of sudden death in hypertrophic cardiomyopathy. Circulation 2010;121:445–56.

125. Ommen SR, Maron BJ, Olivotto I, et al. Long-term effects of surgical septal myectomy on survival in patients with obstructive hypertrophic cardiomyopathy. J Am Coll Cardiol 2005;46: 470–6.

KEY WORDS cardiovascular imaging, echocardiography, heart failure, hypertrophic cardiomyopathy, magnetic resonance imaging, sudden death